Theory of the two step enantiomeric purification of 1,3 dimethylallene

David Gerbasi and Paul Brumer[a)]
Chemical Physics Theory Group, Department of Chemistry, The University of Toronto, 80 St. George Street, Toronto, M5S3H6, Canada

Ioannis Thanopulos, Petr Král, and Moshe Shapiro
Department of Chemical Physics, The Weizmann Institute of Science, Rehovot, 76100, Israel

(Received 12 November 2003, accepted 1 April 2004)

An application of a recently proposed [P. Král *et al.*, Phys. Rev. Lett. **90**, 033001 (2003)] two step optical control scenario to the purification of a racemic mixture of 1,3 dimethylallene is presented. Both steps combine adiabatic and diabatic passage phenomena. In the first step, three laser pulses of mutually perpendicular linear polarizations, applied in a ''cyclic adiabatic passage'' scheme, are shown to be able to distinguish between the *L* and *D* enantiomers due to their difference in matter-radiation phase. In the second step, which immediately follows the first, a sequence of pulses is used to convert one enantiomer to its mirror-imaged form. This scenario, which only negligibly populates the first excited electronic state, proves extremely useful for systems such as dimethylallene, which can suffer losses from dissociation and internal conversion upon electronic excitation. We computationally observe conversion of a racemic mixture of dimethylallene to a sample containing ≈95% of the enantiomer of choice.
[DOI: 10.1063/1.1753552]

I. INTRODUCTION

Chiral purification, which generally involves an asymmetric catalyst and is important for many chemical reactions, has proven to be a challenging endeavor for synthetic chemists and biochemists.[1] In recent years, the idea of controlling the enantiomeric excess via quantum methods has also been of interest. Specifically, several laser schemes have been proposed to convert an initial racemic mixture of chiral molecules to one where the concentration of a particular enantiomer has been greatly enhanced.[2–9] Amongst these efforts is the work of Fujimura and co-workers who make use of linearly polarized light sources to enhance the enantiomeric concentration of both preoriented and randomly oriented samples of H_2POSH,[4] of González *et al.* who use sequences of π pulses and adiabatic transitions to control the enantiomeric concentrations of H_2POSH,[5] and of Salam and Meath who have demonstrated enantiomeric excess with the use of circularly polarized light sources of varying durations.[6] We have shown that a laser scenario, aptly called ''laser distillation,'' which makes use of three linearly perpendicular laser pulses in a randomly oriented sample, is capable of chiral purification.[8] Preliminary application of this scenario to the molecule 1,3 dimethylallene showed promising results.[9]

Recently, several of the authors suggested another method for achieving chiral separation by using a two-step enantio-selective optical switch.[10] In the first step, called the ''enantio-discriminator,'' both *L* and *D* enantiomers are excited to each different vibrational state.[11] The approach is akin to the adiabatic passage used to completely transfer population between quantum states that are usually optically coupled as $|1\rangle\leftrightarrow|2\rangle\leftrightarrow|3\rangle$. However, since chiral molecules have ill-defined parity, it is possible to close the cycle by introducing a third field which couples the states $|1\rangle\leftrightarrow|3\rangle$. The interference of one and two photon transitions along the two paths renders the evolution dependent on the total phase Θ of the three coupling terms. Since the transition dipoles of the two enantiomers differ in sign, the evolution of the two under the action of the three fields is different, and the enantiomers can be separated. In the second step, called the ''enantio-converter,'' which immediately follows the first, one of the enantiomers is converted to its mirror-image. The transfer is realized by simultaneously introducing two dump pulses, followed, after a delay, by two pump pulses and is based on a new multipath transfer technique.[12] In total, four vibrational eigenstates are necessary for the transfer to be realized. An alternative method, described below, selects eigenstates in the first excited electronic state to be sufficiently close in energy such that a single pump and dump pulse is sufficient to realize the population transfer, eliminating the need to use four lasers. It would also be feasible to use chirped pulses to reduce the number of lasers, however, a greater number of eigenstates might be involved in the transfer process, adding a degree of complexity that we would like to avoid. Thus, in just two steps, the racemic mixture of chiral molecules can be greatly enhanced into the enantiomer of choice.

It is the intent of this paper to apply this two step chiral purification method to the realistic molecule 1,3 dimethylallene. Specifically, in Sec. II, a detailed review of the first step, the ''enantio-discriminator,'' is presented with the important addition of the rotational degree of freedom. Next, in Sec. III, the second step ''enantio-converter'' is modified. Here only two laser pulses, one pump and one dump pulse, is used instead of the four pulses originally proposed. Note that the dynamics in both steps is sufficiently described in the

a)Electronic mail: pbrumer@tikva.chem.utoronto.ca

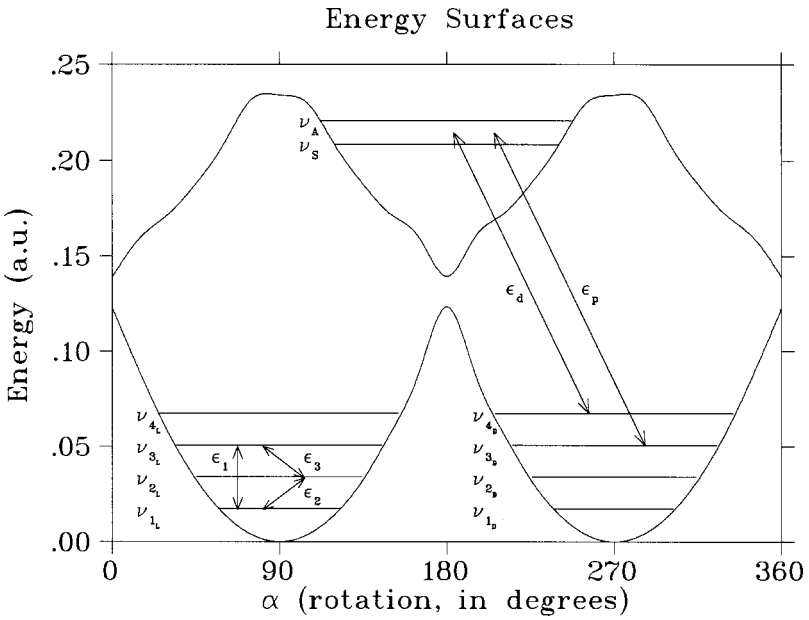

FIG. 1. Two step excitation scheme as described in text. An initial sequence of pulses discriminates between *L* and *D* enantiomers by a closed loop STIRAP (3 laser scheme shown in bottom of ground state potential energy surface). This is followed by an adiabatic passage multi path transfer of enantiomeric population by a "pump", ϵ_p, and "dump", ϵ_d, pulse. Note that all lasers operate on both *L* and *D* enantiomer since $E_D \approx E_L$. Hence ϵ_1, ϵ_2, and ϵ_3 shown only on the left operate as well on the right enantiomer. Similarly, ϵ_p and ϵ_d, shown only on the right, operate on the left enantiomer as well. Also note that only the vibrational levels are shown here; their associated rotational levels are described in the text.

rotating wave approximation because of the use of resonant transitions. Lastly, results demonstrating the validity of this two step process along with a discussion and conclusion are presented in Sec. IV.

II. ENANTIO-DISCRIMINATOR

A. Three-level cyclic population transfer

Consider three vibrational levels in the ground electronic state of a racemic mixture, denoted by $|\nu_i\rangle_{L,D}$, $i=1, 2, 3$, where $E_D \approx E_L$. We operate on the system with three laser pulses in a "counterintuitive" order. That is, we start with a "dump" pulse ϵ_3 that couples the states $|\nu_2\rangle \leftrightarrow |\nu_3\rangle$ followed, after a delay of 2α, where α is the pulse width, by two simultaneous "pump" pulses ϵ_1 and ϵ_2 that couple states $|\nu_1\rangle \leftrightarrow |\nu_3\rangle$ and $|\nu_1\rangle \leftrightarrow |\nu_2\rangle$, respectively, see Fig. 1. The external electric field is then given by

$$\mathbf{E}(t) = \sum_{k=1,2,3} \mathbf{E}_k(t) \equiv \sum_{k=1,2,3} 2\hat{\epsilon}_k \,\mathrm{Re}[\varepsilon_k(t)\exp(i\omega_k t + i\delta_k)], \tag{1}$$

where $\varepsilon_k(t)$ is the pulse envelope, ω_k is the central laser frequency, δ_k is the relative phase, and $\hat{\epsilon}_k$ is the polarization direction.

The dynamics of the system in the presence of radiation is described by the time dependent Schrödinger equation, in the rotating wave approximation, by

$$\dot{\mathbf{c}}(t) = i\mathbf{H}(t)\cdot\mathbf{c}(t), \tag{2}$$

where the effective Hamiltonian $\mathbf{H}(t)$ is given by

$$\mathbf{H}(t) = \begin{bmatrix} 0 & \Omega_{12} & \Omega_{13} \\ (\Omega_{12})^* & 0 & \Omega_{23} \\ (\Omega_{13})^* & (\Omega_{23})^* & 0 \end{bmatrix}. \tag{3}$$

Here $\mathbf{c}=(c_1,c_2,c_3)^T$, $\Omega_{ij}(t) \equiv \chi_{ij}\exp(i\Delta_{ij}t)\exp(i\delta_k)/\hbar$, $\chi_{ij} \equiv \mu_{ij}\varepsilon_k(t)$ are the Rabi frequencies, $\Delta_{ij} \equiv \omega_k - \omega_{ij}$, $\mu_{ij} \equiv \langle i|\boldsymbol{\mu}_k|j\rangle$, with $i=1, 2$, $j=2, 3$, and $k=1, 2, 3$.

By considering the eigenvalues of the Hamiltonian of Eq. (3), given by

$$E_0 = \frac{2^{1/3}a}{3c} + \frac{c}{3\cdot 2^{1/3}},$$
$$E_{-,+} = \frac{-(1\pm i\sqrt{3})a}{3\cdot 2^{1/3}c} - \frac{(1\mp i\sqrt{3})c}{6\cdot 2^{1/3}}, \tag{4}$$

where

$$a = 3(|\Omega_{12}|^2 + |\Omega_{13}|^2 + |\Omega_{23}|^2),$$
$$b = 3^3 2\ \mathrm{Re}\,\Xi, \tag{5}$$
$$c = [b + \sqrt{b^2 + 4(-a)^3}]^{1/3},$$

with $\Xi = \Omega_{12}\Omega_{13}\Omega_{23}^* \equiv \mu_{12}\mu_{13}\mu_{23}^*\varepsilon_1\varepsilon_2\varepsilon_3^*\Theta$, we see that the three eigenvalues depend only on the overall phase Θ of Ξ which is composed of a time independent (optical) part, $\varphi = \delta_1 + \delta_2 - \delta_3$, and a time dependent (material) part, $\Sigma t = (\Delta_{12} + \Delta_{13} - \Delta_{23})t$. Since the phase of both enantiomers differ by π, it is possible to choose the phase of the optical fields such that $\Theta = \vartheta$, where ϑ is an arbitrary phase, for one enantiomer and, inevitably, $\Theta = \vartheta + \pi$ for the other. Therefore, the population, which has been following the initial adiabatic level $|E_0\rangle$ in both enantiomers, goes at $t=\alpha$, where α is the pulse width, smoothly through the crossing region and *diabatically* transfers to either the $|E_-\rangle$ or the $|E_+\rangle$ states, depending on whether $\Theta = \vartheta$ or $\Theta = \vartheta + \pi$. After the crossing is complete, $t > \alpha$, the process becomes adiabatic again, with the enantiomer population residing fully in either $|E_-\rangle$ or $|E_+\rangle$.[11]

B. Rotational considerations

Each vibrational state is associated with an asymmetric top wave function of the form[9]

$$\langle \phi,\theta,\chi|J,M\rangle^{\tau} \equiv \Psi^{\tau}_{J,M}(\phi,\theta,\chi) = \left(\frac{2J+1}{8\pi^2}\right)^{1/2} \sum_{\lambda} a_{\lambda,\tau} D^{J}_{\lambda,M}(\phi,\theta,\chi), \quad (6)$$

which are linear combinations of rotational matrices given in Edmonds notation[13] with (ϕ,θ,χ) denoting the three Euler angles. The parameter λ is the projection of the total angular momentum on the space fixed frame, M is the projection of the total angular momentum on the molecular frame, and τ is defined as $\tau=\lambda_{-1}-\lambda_1$, where λ_{-1} is the value of $|\lambda|$ the top would approach in the limit of a prolate top and λ_1 is the value of $|\lambda|$ the top would approach in the limit of an oblate top.

The dipole operator, relating the space fixed frame to the molecular frame, is given by[8,9]

$$\mu_l \equiv \boldsymbol{\mu}_l \cdot \hat{\boldsymbol{\epsilon}}_l = f_l t_{q_l} \sum_{k=-1}^{k=1} \mu_l^{(k)} \{ D^1_{k,q_l}(\phi,\theta,\chi) + p_l(-1)^{q_l} D^1_{k,-q_l}(\phi,\theta,\chi)\}, \quad (7)$$

where

$$\mu_l^{(+1)} = -\frac{1}{\sqrt{2}}(\mu_l^x + i\mu_l^y), \quad \mu_l^{(0)} = \mu_l^z, \quad \mu_l^{(-1)} = \frac{1}{\sqrt{2}}(\mu_l^x - i\mu_l^y), \quad (8)$$

and $t_0=1/2$ and $t_1=1/\sqrt{2}$. Depending on the space fixed orientation of the pulse, $f_l=1$, $q_l=0$, and $p_l=1$ for Z polarization, $f_l=-1$, $q_l=1$, and $p_l=1$ for X polarization, and $f_l=i$, $q_l=1$, and $p_l=-1$ for Y polarization. Here $\hat{\boldsymbol{\epsilon}}_1$ is polarized along the X axis, $\hat{\boldsymbol{\epsilon}}_2$ along the Y axis, and $\hat{\boldsymbol{\epsilon}}_3$ along the Z axis. Note that the three fields must be perpendicular to one another in order to maintain control upon angular averaging.[8]

It is difficult, if not impossible, to realize the three level scenario of Král *et al.*, shown above, once one includes rotational contributions. This is because dimethylallene is a near symmetric top and the energy degeneracy in the λ quantum number, found in symmetric tops, is only slightly removed. Therefore even though the bandwidth of the pulses are relatively small, there are rotational levels that are separated by $\approx 0.03\ \mathrm{cm}^{-1}$. In addition, due to the perpendicular polarizations, all M levels that are in accord with the selection rule $\Delta M=0,\ \pm 1$ are excited. In total, by including all levels under the bandwidth of the pulses, we need to include five vib-rotational wave functions of the form

$$|1\rangle = |\nu_1, J=0, M=0\rangle^{\tau=0}, \quad (9)$$

$$|2\rangle = |\nu_2, J=1, M=0\rangle^{\tau=0}, \quad (10)$$

$$|3\rangle = |\nu_2, J=1, M=0\rangle^{\tau=+1}, \quad (11)$$

$$|4\rangle = |\nu_3, J=1, M=-1\rangle^{\tau=-1}, \quad (12)$$

$$|5\rangle = |\nu_3, J=1, M=+1\rangle^{\tau=-1}, \quad (13)$$

in the overall enantio-discriminator scheme. Note that we have assumed that the initial population resides in the ground vib-rotational state. However, the enantio-discriminator process remains valid for different choices of initial J states. Here initial $J=0$ was chosen in order to simplify the computation.

The overall process now works as follows: The "dump" pulse $\boldsymbol{\epsilon}_3$ first couples states $|\nu_2,J,M\rangle^{\tau} \leftrightarrow |\nu_3,J,M\rangle^{\tau}$ followed, after a delay of 2α, by two "pump" pulses $\boldsymbol{\epsilon}_1$ and $\boldsymbol{\epsilon}_2$ coupling states $|\nu_1,J,M\rangle^{\tau} \leftrightarrow |\nu_2,J,M\rangle^{\tau}$ and $|\nu_1,J,M\rangle^{\tau} \leftrightarrow |\nu_3,J,M\rangle^{\tau}$, respectively. The central frequency of $\varepsilon_1(t)$ is chosen near-resonant with the transition between states $|\nu_1,J=0,M=0\rangle^{\tau=0}$ and $|\nu_3,J=1,M=\pm 1\rangle^{\tau=-1}$, $\varepsilon_2(t)$ is chosen near-resonant with the $|\nu_1,J=0,M=0\rangle^{\tau=0}$ to $|\nu_2,J=1,M=0\rangle^{\tau=0,+1}$ transition, and $\varepsilon_3(t)$ is chosen near-resonant with the transition between $|\nu_2,J=1,M=0\rangle^{\tau=0,+1}$ and $|\nu_3,J=1,M=\pm 1\rangle^{\tau=-1}$.

Making use of the rotating wave approximation, the dynamics of the five level vib-rotational system in the presence of radiation is described by the time dependent Schrödinger equation, Eq. (2), with an effective Hamiltonian $\mathbf{H}(t)$ given by

$$\mathbf{H}(t) = \begin{bmatrix} 0 & \Omega_{12} & \Omega_{13} & \Omega_{14} & \Omega_{15} \\ (\Omega_{12})^* & 0 & 0 & \Omega_{24} & \Omega_{25} \\ (\Omega_{13})^* & 0 & 0 & \Omega_{34} & \Omega_{35} \\ (\Omega_{14})^* & (\Omega_{24})^* & (\Omega_{34})^* & 0 & 0 \\ (\Omega_{15})^* & (\Omega_{25})^* & (\Omega_{35})^* & 0 & 0 \end{bmatrix}. \quad (14)$$

Here $\mathbf{c}=(c_1,c_2,c_3,c_4,c_5)^T$ and the notation is a natural extension of that previously introduced [Eq. (3)]. Note that the interplay between vibrational levels in Eq. (14) is clearly seen by referring to Eqs. (9)–(13).

By diagonalizing the Hamiltonian of Eq. (14), one can show that the system evolution is once again dependent on the total phase Θ which is composed of a time independent part $\varphi=\delta_1+\delta_2-\delta_3$ and a time dependent part $\Sigma t=(\Delta_{i,j}+\Delta_{k,l}-\Delta_{m,n})t$. Here $\Delta_{i,j}$ is the detuning from $\boldsymbol{\epsilon}_1$ (e.g., either $\Delta_{1,2}$ or $\Delta_{1,3}$), $\Delta_{k,l}$ is the detuning from $\boldsymbol{\epsilon}_2$, and $\Delta_{m,n}$ is the detuning from $\boldsymbol{\epsilon}_3$. At first glance it would seem that the phase control we previously had in the three level system no longer exists because the overall phase differs for a given set of vib-rotational eigenstates. However, we note that since states $|4\rangle$ and $|5\rangle$ are degenerate, detuning to either of these states will be the same, i.e., $\Delta_{1,4}=\Delta_{1,5}$, etc. It is also possible to tune the central laser frequencies of $\boldsymbol{\epsilon}_2$ and $\boldsymbol{\epsilon}_3$ such that $\Delta_{2,4}\equiv\Delta_{3,4}$ and $\Delta_{2,5}\equiv\Delta_{3,5}$. In doing so, the dynamics of this five level system resembles that of the original three level system insofar that they have the same components in the overall phase. Therefore, by choosing the phase of the optical fields such that $\Theta=\vartheta$ for one enantiomer, the other is inevitably $\Theta=\vartheta+\pi$ subsequently leading to their totally different dynamics. Specifically, both enantiomers begin by *adiabatically* following the initial state. At $t=\alpha$, they smoothly go through the crossing region and *diabatically* transfer population to each different state, depending on the identity of the enantiomer, i.e., its overall phase. After the

TABLE I. Laser pulse parameters for the two-step enantiomeric control of dimethylallene where β is the field strength, α the pulse width, ω the transition frequency, and Δ the detunings.

Laser pulse	β (W/cm^2)	α (ns)	ω (cm^{-1})	Δ (cm^{-1})	Polarization
Step 1					
ϵ_1	5.116×10^{6}	1.70	1232	1.5×10^{-3}	X
ϵ_2	4.527×10^{8}	1.70	407	-1.5×10^{-3}	Y
ϵ_3	3.823×10^{4}	1.70	825	-1.5×10^{-3}	Z
Step 2					
ϵ_p	3.509×10^{10}	1.20	50 131	1.85×10^{-1}	X
ϵ_d	5.614×10^{11}	1.20	49 869	1.85×10^{-1}	X

TABLE II. Values of transition dipole matrix elements $\mu_{ij}\equiv\langle i|\mu|j\rangle$ between vibrational levels in units of Debye.

$\mu_{12}=5.59\times10^{-2}$,	$\mu_{3S}=4.28\times10^{-3}$
$\mu_{13}=5.29\times10^{-3}$,	$\mu_{4A}=2.37\times10^{-3}$
$\mu_{23}=6.54\times10^{-2}$,	$\mu_{4S}=1.78\times10^{-3}$
$\mu_{3A}=5.01\times10^{-3}$,	

crossing is complete, the process becomes adiabatic once again and each enantiomer population resides in a different state.

III. ENANTIO-CONVERTER

A. Six level transfer process

Assuming that the L enantiomer has been excited to vibrational level $|\nu_3\rangle_L$, we now proceed to convert it to its mirror-image in the $|\nu_4\rangle_D$ state by going through a linear superposition of states $|\nu_S\rangle$ and $|\nu_A\rangle$, while leaving the other unaffected, see Fig. 1.

This process is based on a new multipath transfer technique,[12] however, here, only two parallel lasers are applied polarized in the X direction, contrary to the original four laser scheme.[10] Specifically, one ''dump'' pulse couples both states $|\nu_S\rangle$ and $|\nu_A\rangle$ to states $|\nu_4\rangle_{L,D}$ and is followed simultaneously by one ''pump'' pulse, after a delay of 2α, which couples each of the $|\nu_S\rangle$ and $|\nu_A\rangle$ states to states $|\nu_3\rangle_{L,D}$. Note that since the pulses are on a nanosecond time scale, a requirement for adiabatic passage, the excited state's energies need to be very close together for this two laser scheme to be effective. This criteria can be satisfied by the correct choice of vibrational and rotational energy levels, as seen below. For large energy spacings, chirped pulses can be used. However, in that case, several other eigenstates might be included in the transfer process, which can prove to be quite computationally cumbersome.

The overall ''enantio-converter'' Hamiltonian matrix is then given by

$$\mathbf{H}(t)=\begin{bmatrix} 0 & 0 & \Omega_{3_LS} & \Omega_{3_LA} & 0 & 0 \\ 0 & 0 & \Omega_{3_DS} & \Omega_{3_DA} & 0 & 0 \\ (\Omega_{3_LS})^* & (\Omega_{3_DS})^* & 0 & 0 & (\Omega_{4_LS})^* & (\Omega_{4_DS})^* \\ (\Omega_{3_LA})^* & (\Omega_{3_DA})^* & 0 & 0 & (\Omega_{4_LA})^* & (\Omega_{4_DA})^* \\ 0 & 0 & \Omega_{4_LS} & \Omega_{4_LA} & 0 & 0 \\ 0 & 0 & \Omega_{4_DS} & \Omega_{4_DA} & 0 & 0 \end{bmatrix}, \tag{15}$$

where $c(t)=(c_{3_L},c_{3_D},c_S,c_A,c_{4_L},c_{4_D})$. All other terms are a natural extension of the first step [Eq. (3)]. The Hamiltonian matrix above has four nonzero eigenvalues and two null eigenvalues that correspond to two dark states with coefficients $\mathbf{c}_1(t)=(-d_+,-d_-,0,0,2\Omega_{3_LS},0)$, $\mathbf{c}_2(t)=(-d_-,-d_+,0,0,0,2\Omega_{3_LS})$, where $d_\pm=\Omega_{4_LS}\pm r\Omega_{4_LA}$, with $r\equiv\Omega_{3_LS}/\Omega_{3_LA}$. These expressions show that the system can follow two possible paths, where only *one* of them is flipping the symmetry of the initial state.

Consider the situation where, for simplicity, $r=1$ and $r'=\Omega_{4_LS}/\Omega_{4_LA}=1$, at the beginning of the process only the dark state $\mathbf{c}_1(t_{\rm ini})=(1,0,0,0,0,0)$ correlates with the initial state $|\nu_3\rangle_L$. At the end of the process, this dark state correlates with the vector $\mathbf{c}_1(t_{\rm end})=(0,0,0,0,1,0)$ for the $|\nu_4\rangle_L$ state, so the symmetry is preserved. On the other hand, if we flip the phase of just one of the Rabi frequencies of either the dump or pump pulse, the system follows the dark state $\mathbf{c}_2$, which correlates at the end with the state $\mathbf{c}_2(t_{\rm end})=(0,0,0,0,0,1)$. The final population thus occupies the $|\nu_4\rangle_D$ state, with the opposite symmetry. Therefore, for a specific overall phase Θ, the state $|\nu_3\rangle_L$ can be excited to either state $|\nu_4\rangle_L$ or state $|\nu_4\rangle_D$ by changing Θ by a factor of π.

B. Rotational considerations

Once again, each vibrational wave function is associated with an asymmetric top wave function given by Eq. (6). The rotational components for states $|\nu_3\rangle_{L,D}$, as well for states $|\nu_4\rangle_{L,D}$, are the same as in the first step [Eqs. (12) and (13)]. The chosen rotational wave functions for $|\nu_S\rangle$ and $|\nu_A\rangle$ are $|J=2,M=0\rangle^{\tau=-2}$ and $|J=0,M=0\rangle^{\tau=0}$, respectively. The reason being that the energy separation between the states $|\nu_S,J=2,M=0\rangle^{\tau=-2}$ and $|\nu_A,J=0,M=0\rangle^{\tau=0}$ is ≈0.1

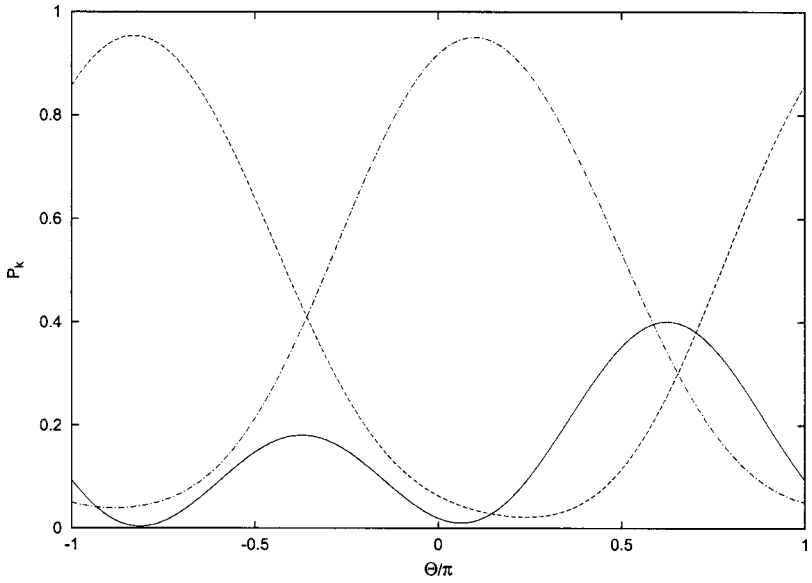

FIG. 2. Final population of states $|\nu_1\rangle_L$ (solid line), $|\nu_2\rangle_L$ (dash-dash line), and $|\nu_3\rangle_L$ (dot-dash line) as a function of overall phase Θ. The corresponding populations for the *D* enantiomer are shifted by a factor of π.

cm^{-1}, guaranteeing that a single pump and dump pulse is sufficient to realize the population transfer. The complete set of vib-rotational levels is then given by

$$
\begin{aligned}
|1\rangle &= |\nu_3, J=1, M=-1\rangle_L^{\tau=-1},\\
|2\rangle &= |\nu_3, J=1, M=+1\rangle_L^{\tau=-1},\\
|3\rangle &= |\nu_3, J=1, M=-1\rangle_D^{\tau=-1},\\
|4\rangle &= |\nu_3, J=1, M=+1\rangle_D^{\tau=-1},\\
|5\rangle &= |\nu_S, J=2, M=0\rangle^{\tau=-2},\\
|6\rangle &= |\nu_A, J=0, M=0\rangle^{\tau=0},
\end{aligned}
\tag{16}
$$

$$
\begin{aligned}
|7\rangle &= |\nu_4, J=1, M=-1\rangle_L^{\tau=-1},\\
|8\rangle &= |\nu_4, J=1, M=+1\rangle_L^{\tau=-1},\\
|9\rangle &= |\nu_4, J=1, M=-1\rangle_D^{\tau=-1},\\
|10\rangle &= |\nu_4, J=1, M=+1\rangle_D^{\tau=-1}.
\end{aligned}
$$

The laser setup is the same as above, with two parallel lasers polarized in the *X* direction. Note that there is no need to impose a sense of direction because the enantiomers are distinguishable after the first step. Consequently, angular averaging does not remove any of the control. The effective Hamiltonian matrix is given by

$$
\mathbf{H}(t) = \begin{bmatrix}
0 & 0 & 0 & 0 & \Omega_{1,5} & \Omega_{1,6} & 0 & 0 & 0 & 0\\
0 & 0 & 0 & 0 & \Omega_{2,5} & \Omega_{2,6} & 0 & 0 & 0 & 0\\
0 & 0 & 0 & 0 & \Omega_{3,5} & \Omega_{3,6} & 0 & 0 & 0 & 0\\
0 & 0 & 0 & 0 & \Omega_{4,5} & \Omega_{4,6} & 0 & 0 & 0 & 0\\
(\Omega_{1,5})^* & (\Omega_{2,5})^* & (\Omega_{3,5})^* & (\Omega_{4,5})^* & 0 & 0 & (\Omega_{7,5})^* & (\Omega_{8,5})^* & (\Omega_{9,5})^* & (\Omega_{10,5})^*\\
(\Omega_{1,6})^* & (\Omega_{2,6})^* & (\Omega_{3,6})^* & (\Omega_{4,6})^* & 0 & 0 & (\Omega_{7,6})^* & (\Omega_{8,6})^* & (\Omega_{9,6})^* & (\Omega_{10,6})^*\\
0 & 0 & 0 & 0 & \Omega_{7,5} & \Omega_{7,6} & 0 & 0 & 0 & 0\\
0 & 0 & 0 & 0 & \Omega_{8,5} & \Omega_{8,6} & 0 & 0 & 0 & 0\\
0 & 0 & 0 & 0 & \Omega_{9,5} & \Omega_{9,6} & 0 & 0 & 0 & 0\\
0 & 0 & 0 & 0 & \Omega_{10,5} & \Omega_{10,6} & 0 & 0 & 0 & 0
\end{bmatrix},
\tag{17}
$$

where $c(t)=(c_1,c_2,c_3,c_4,c_5,c_6,c_7,c_8,c_9,c_{10})$. All other terms are a natural extension of the first step [Eq. (3)].

Similar to the six level vibrational case above, the dynamics of the system can either follow one of two dark states where one is symmetry preserving and the other symmetry changing. Therefore, control of the transfer of population from one enantiomer to the other is feasible, for a given overall phase Θ, and enantiomeric purification is realized.

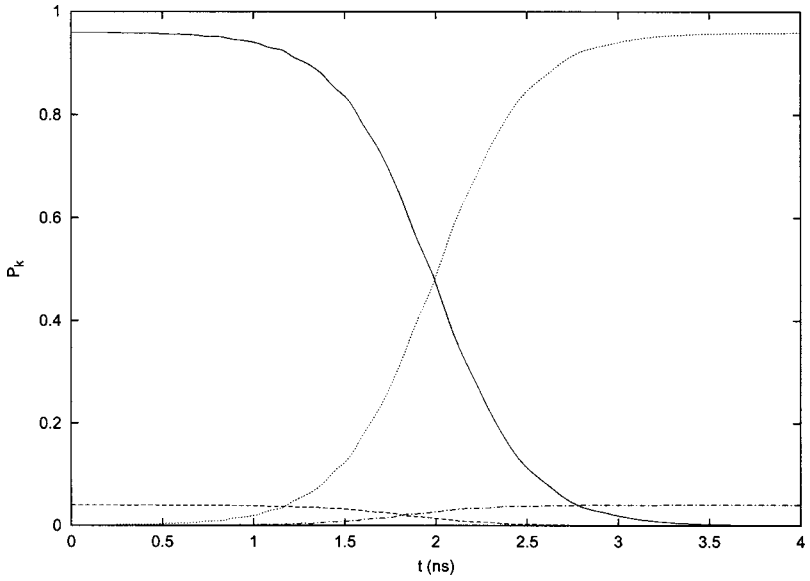

FIG. 3. Final population of states $|\nu_3\rangle_L$ (solid line), $|\nu_3\rangle_D$ (dash-dash line), $|\nu_4\rangle_L$ (dash-dot line), $|\nu_4\rangle_D$ (dot-dot line), $|\nu_5\rangle$ (double dash-dot line), and $|\nu_6\rangle$ (triple dash-dot line) for the enantio-converter scheme as a function of time. Note that the states $|\nu_5\rangle$ and $|\nu_6\rangle$ are never significantly populated.

IV. RESULTS AND CONCLUSION

In order to realize this two step process, we make use of Gaussian pulses of the form $\epsilon_\ell = \beta_\ell \exp\{-[(t-t_\ell)/\alpha_\ell]^2\}$ where β_ℓ is the field strength and α is the pulse width. The specific laser parameters are given in Table I. The values for the transition dipole moments, given in Table II, are obtained using results from a previous two-dimensional molecular structure computation[14] and utilizing a discrete variable representation (DVR) computation.[15] In general, the transition dipole moments are rather weak, on the order of 10^{-2} to 10^{-3} D for the first step and require field intensities no stronger than $\approx 5\times 10^8$ W/cm^2. Note that choosing vibrational levels such that the transition frequencies are on the order of 20 000 cm^{-1} is also possible for realizing the enantiomer discrimination step, but these transitions have weaker transition dipole moments and would require stronger field intensities. The second step transition dipole moments are an order of magnitude weaker than the first and consequently require stronger field intensities, $\approx 5\times 10^{11}$ W/cm^2. By setting the overall phase to 0.100 rad, 95.06% of the L enantiomer has been excited to state $|\nu_3\rangle_L$. At the same time, 93.68% of the D enantiomer has been transfered to state $|\nu_2\rangle_D$ with only 3.95% excited to state $|\nu_3\rangle_D$ since its overall dynamics differ by a factor of π relative to the L enantiomer, see Fig. 2. Note here that only the final population in each vibrational state is given. That is, the population of $|\nu_3\rangle_L$ is in reality the sum of $|\nu_3, J=1, M=-1\rangle_L^{\tau=-1}$ and $|\nu_3, J=1, M=+1\rangle_L^{\tau=-1}$. The same holds true for the other populations. At first glance, it would seem that the discrimination step is not as robust as reported by Král and Shapiro,[11] however, the difference achieved between $|\nu_3\rangle_D$ and $|\nu_3\rangle_L$ is nonetheless impressive. The differences can be attributed to the fact that not all of the Rabi frequencies are the same, hence giving slightly different dynamics.

In the laboratory implementation, one would envision using a phase stabilized cw source at one of the frequencies of interest, say ω_{12}, to seed a nonlinear crystal, which, like in an optical parametric amplifier, given an ω_{13} pulse, will in addition to an ω_{12} pulse, generate (by difference-frequency mixing) the ω_{23} pulse. By changing the phase of the cw seed light, we can make sure that the sum of the three phases (the ''phase sum'') of the three pulses is controllable. Therefore, by monitoring the product formation, it is possible to determine the overall phase that would give the maximum enentiomer yield. If we see that we are purifying the unwanted enantiomer, we can then give the seed light a phase shift of π to produce the desired one.

Once the above process is complete, we proceed to transfer population from one enantiomer to the other. As opposed to the first step, the enantio-converter step is very robust and resembles the same four level system as the original scheme insofar as there are only four different magnitudes of Rabi frequencies. This allows for 100% conversion between the D and L enantiomers. As shown in Fig. 3, all of the L population excited to $|\nu_3\rangle_L$ in the first step is completely transfered to $|\nu_4\rangle_D$. However, the initial population from the $|\nu_3\rangle_D$ is also converted to $|\nu_4\rangle_L$. Therefore, the final population in both D and L is 95.55% and 4.45% respectively. Note that if one would rather enhance the population of the L enantiomer, one turns the laboratory ''knob'' such that the overall phase changes by a factor of π. Note also, as is evident from Fig. 3, that none of the population ever significantly occupies the states $|\nu_5\rangle$ and $|\nu_6\rangle$. Therefore, there is no concern about possible dissociation from internal conversion as was the case with previous scenarios involving the enantiomeric control of dimethylallene[9] which proceed via the excited state. In this case it is only necessary to ensure that the dynamical evolution of the system be faster than the decoherence time attributed to collisional dephasing.

These results show that using this scenario to enhance the enantiomeric excess is computationally feasible. Experimentally, however, it requires the use of several lasers. If a reduction in the number of lasers is necessary then one alternative is to stop the process before the enantio-conversion. That is, since both enantiomers are different as a result of the first step, they can be physically separated[11] in lieu of the second step. This will, however, eliminate half the sample

population, but enantiomeric purification will have nonetheless occurred.

ACKNOWLEDGMENT

This project was supported by the U.S. Office of Naval Research, the EU IHP program HPRN-CT-1999-00129, and the Swiss Friends of the Weizmann Institute.

[1] R. Noyori, in *Asymmetric Catalysis in Organic Synthesis* (Wiley-Interscience, New York, 1994).
[2] M. Shapiro and P. Brumer, in *Principles of the Quantum Control of the Molecular Processes* (Wiley-Interscience, New York, 2003).
[3] M. Shapiro, E. Frishman, and P. Brumer, Phys. Rev. Lett. **84**, 1669 (2000).
[4] K. Hoki, Y. Ohtsuki, and Y. Fujimura, J. Chem. Phys. **114**, 1575 (2001); K. Hoki, L. González, and Y. Fujimura, *ibid.* **116**, 2433 (2002); Y. Ohta, K. Hoki, and Y. Fujimura, *ibid.* **116**, 7509 (2002); K. Hoki, L. González, and Y. Fujimura, *ibid.* **116**, 8799 (2002); K. Hoki, D. Kröner, and J. Manz, Chem. Phys. **267**, 59 (2001).
[5] L. González, D. Kröner, and I. R. Solá, J. Chem. Phys. **115**, 2519 (2001); D. Kröner, M. F. Shibl, and L. González, Chem. Phys. Lett. **372**, 242 (2003); Y. Fujimura, L. González, K. Hoki, D. Kröner, J. Manz, and Y. Ohtsuki, Angew. Chem., Int. Ed. Engl. **39**, 4586 (2000).
[6] A. Salam and W. J. Meath, Chem. Phys. **228**, 115 (1998); J. Chem. Phys. **106**, 7865 (1997).
[7] D. Gerbasi, M. Shapiro, and P. Brumer, J. Chem. Phys. **115**, 5349 (2001).
[8] E. Frishman, M. Shapiro, D. Gerbasi, and P. Brumer, J. Chem. Phys. **119**, 7237 (2003).
[9] D. Gerbasi, M. Shapiro, and P. Brumer (unpublished).
[10] P. Král, I. Thanopulos, M. Shapiro, and D. Cohen, Phys. Rev. Lett. **90**, 033001 (2003).
[11] P. Král and M. Shapiro, Phys. Rev. Lett. **87**, 183002 (2001).
[12] P. Král, Z. Amitay, and M. Shapiro, Phys. Rev. Lett. **89**, 063002 (2002).
[13] A. R. Edmonds, in *Angular Momentum in Quantum Mechanics*, 2nd ed. (Princeton University Press, Princeton, 1960).
[14] E. Deretey, M. Shapiro, and P. Brumer, J. Phys. Chem. A **105**, 9509 (2001).
[15] D. T. Colbert and W. H. Miller, J. Chem. Phys. **96**, 1982 (1992).